



HAL
open science

Interaction of reed and acoustic resonator in clarinetlike systems

Fabrice Silva, Jean Kergomard, Christophe Vergez, Joël Gilbert

► **To cite this version:**

Fabrice Silva, Jean Kergomard, Christophe Vergez, Joël Gilbert. Interaction of reed and acoustic resonator in clarinetlike systems. 2008. hal-00197147v1

HAL Id: hal-00197147

<https://hal.science/hal-00197147v1>

Preprint submitted on 7 Mar 2008 (v1), last revised 16 Oct 2008 (v2)

HAL is a multi-disciplinary open access archive for the deposit and dissemination of scientific research documents, whether they are published or not. The documents may come from teaching and research institutions in France or abroad, or from public or private research centers.

L'archive ouverte pluridisciplinaire **HAL**, est destinée au dépôt et à la diffusion de documents scientifiques de niveau recherche, publiés ou non, émanant des établissements d'enseignement et de recherche français ou étrangers, des laboratoires publics ou privés.

Interaction of reed and acoustic resonator in clarinet-like systems

Fabrice Silva, Jean Kergomard, and Christophe Vergez^{a)}

Laboratoire de Mécanique et d'Acoustique UPR CNRS 7051, 13402 Marseille cedex 20, France

Joël Gilbert^{b)}

Laboratoire d'Acoustique de l'Université du Maine UMR CNRS 6613, 72085 Le Mans cedex 9, France

(Dated: December 14, 2007)

Sound emergence in clarinet-like instruments is investigated in this paper in terms of instability of the static regime. Various models of a reed coupled to a resonator are indeed considered, from the pioneering work of Wilson and Beavers to more recent modelling including refinements such as visco-thermal bore losses, vena contracta at the reed inlet, and reed motion induced flow. Within the framework of linear stability, the pressure threshold above which the model may oscillate as well as the frequency of oscillation at threshold are calculated. The main conclusions confirm that the reed damping plays an important role in the instrument functioning: it is deeply involved in the ease of playing (defined as the pressure threshold) and in the selection of the register the instrument will play on, through the interaction of the reed with one precise resonance of the bore. Another result is that the most sophisticated models studied reduce discrepancies between Wilson and Beavers experimental results and theory, but discrepancies still remain concerning the pressure threshold. Finally, analytical approximations of the oscillating solution based on Fourier series expansion are obtained in the vicinity of the threshold of oscillation. This allows to emphasize the conditions which determine the nature of the bifurcation (direct or inverse) through which the note may emerge, with therefore important consequences on the musical playing performances. As an illustration, it is found that the closeness between the oscillation frequency and one resonance frequency of the bore causes a direct bifurcation to occur.

PACS numbers: 43.75.Pq

I. INTRODUCTION

Sound production in the reed wind musical instruments is a result of self-sustained reed oscillation. The mechanical oscillator, the reed, acts as a valve which modulates the air flow entering into the instrument, by opening and closing a narrow slit defined between the tip of the reed itself and the lay of the mouthpiece. The phenomenon thus belongs to the class of flow-induced vibrations, which has been extensively studied both theoretically and experimentally (see, for example, Blevins⁷). Various regimes can occur in such systems: static regime, periodic oscillating regimes, and even complex chaotic behaviours.

A first step to study this kind of oscillators, is to analyse the stability of the trivial solution, the equilibrium position of the reed, in order to find a threshold of instability associated to a set of control parameters defining the embouchure (reed, mouthpiece, and player) and the instrument itself. As an output of the threshold analysis, a mouth pressure threshold can be found. It is relevant from the musical playing performance: an estimation of the threshold value is a first evaluation of the ease of playing. In this paper are firstly investigated theoretically the threshold of instability of the reed of a clarinet-like system by revisiting the important pioneering work of Wilson & Beavers⁴³. Secondly, small oscillations beyond

the instability threshold are considered.

To answer the question whether the reed equilibrium is stable or not, several theoretical methods are available and have been used to study reed wind instruments. Using the feedback loop analogy, it is known as the free oscillation linear stability problem in a closed loop obtained when the nonlinear component of the loop is linearized around the trivial solution. Then the linear stability of the reed can be studied with respect to each resonance of the input impedance of the resonator in frequency domain (see, for example, Refs. 3, 5, 10, 20, 34 and 38 for reed instruments, Ref. 18 for lip-reed instruments and Ref. 19 for a generic type of reeds). Using the dynamical system representation where each resonance of the resonator is described as a simple second order oscillator in time domain, the linear stability analysis involves solving eigenvalue problems and analysing the sign of the eigenvalues real part (see, for example, Refs. 12 for lip-reed instruments and 33 for vocal folds). The theoretical results can then be compared with experimental ones coming from artificial mouth by playing them as gently as possible (see, for example, Refs. 3, 14, 15, 43 for reed instruments; Ref. 12 for lip reed instruments; and Refs. 9, 29, 37 for vibrating vocal folds). The first attempt to derive theoretically the spectrum of reed instruments beyond the instability threshold is due to Worman⁴⁴. His results were at the origin of several works such as Refs. 6, 22, 28.

Despite a rather simple description of physical phenomenon, pioneer theoretical and experimental results concerning mouth pressure and frequency at oscillation threshold were obtained by Wilson & Beavers⁴³, showing the important role of reed damping determining the

^{a)}{silva,kergomard,vergez}@lma.cnrs-mrs.fr

^{b)}joel.gilbert@univ-lemans.fr

clarinet-like or lingual pipe organ-like behaviour.

The theory of Wilson and Beavers (hereafter denoted WB) is presented and discussed in section II. Then model improvements from literature are added in the theory in order to try to reduce discrepancies between WB experiments and the theoretical results (section III). Section IV is devoted to a study of small oscillations beyond the instability threshold according to the direct bifurcation behaviour of the clarinet-like instruments. Finally perspectives are discussed in the conclusion.

II. WILSON AND BEAVERS THEORY

A. Basic physical model

The physical model used by WB is reminded with some comments related to more recent literature. It is based on the description of three separate elements: the reed, the bore and the airflow. The model used here is classical and extremely simplified, but is also proven to be efficient in order to reproduce self sustained oscillations (for sound synthesis examples, see Refs. 23, 35). Additional elements will be discussed in the next section.

Reed

Based upon the fact that reed displacement occurs in the vertical direction mainly without torsion, WB, among many authors, have assumed a single degree of freedom motion. Reed-lip-mouthpiece system is thus modelled as a lumped second-order mechanical oscillator with stiffness per unit area K , damping parameter q_r and natural angular frequency ω_r , driven by the pressure drop $P_m - p(t)$ across the reed, with an inward striking behaviour:

$$\frac{d^2 y}{dt^2} + q_r \omega_r \frac{dy}{dt} + \omega_r^2 (y(t) - y_0) = \frac{\omega_r^2}{K} (p(t) - P_m), \quad (1)$$

$p(t)$, P_m , $y(t)$, y_0 , being the mouthpiece pressure, the blowing pressure, the tip opening (denoted $a(t)$ in WB's paper⁴³) and the tip opening without any pressure difference, respectively. P_m is assumed to be constant.

Avanzini *et al.*² have numerically shown that this lumped model is valid for a small vibration theory where only the interaction between bore resonances and the first flexion mode of the reed is investigated. Measured transfer functions of a reed mounted on a mouthpiece also shows a two degree of freedom response²¹.

Bore

The behaviour of the acoustical resonator is determined by an input impedance relationship between acoustic quantities in the mouthpiece (acoustic pressure $p(t)$ and volume flow $u(t)$, or $P(\omega)$ and $U(\omega)$, respectively, in the frequency domain). WB assumed, for a cylindrical bore representing a simplified clarinet body,

an expression given by Backus³:

$$Z_e(\omega) = \frac{P(\omega)}{U(\omega)} = jZ_c \frac{1}{1 - \frac{j}{2Q}} \tan\left(\frac{\omega L}{c} \left(1 - \frac{j}{2Q}\right)\right), \quad (2)$$

where $j^2 = -1$, c and ρ , L , S and $Z_c = \rho c/S$ are the wave speed in free space, density of air, bore length, bore cross section, and characteristic impedance, respectively. The quality factor Q is assumed by WB to be frequency independent, implying a damping proportional to the frequency.

As it will be seen later, this assumption can be discussed, and improved models will be used, because pressure thresholds are strongly influenced by bore losses (which are directly linked to the value of parameter Q).

Airflow

As noted by Hirschberg²⁵, in the case of clarinet-like instruments, the control of the volume flow by the reed position is due to the existence of a turbulent jet. Indeed, a jet is supposed to form in the mouthpiece (pressure p_{jet}) after flow separation from the walls, at the end of the (very short) reed channel. Neglecting the velocity of air flow in the mouth compared to the jet velocity v_{jet} and assuming a downwards air flow ($v_{\text{jet}} > 0$), the Bernoulli theorem applied between the mouth and the reed channel²⁵ leads to:

$$P_m = p_{\text{jet}} + \frac{1}{2} \rho v_{\text{jet}}^2 \quad \text{where } \rho \text{ is the air density.} \quad (3)$$

Assuming a rectangular aperture of width W and height $y(t)$, the volume flow u across the reed channel can be expressed as follows:

$$u(t) = W y(t) \sqrt{\frac{2}{\rho}} \sqrt{P_m - p_{\text{jet}}(t)}. \quad (4)$$

Since the cross section of the mouthpiece is large compared to the cross section of the reed channel, it can be assumed that all the kinetic energy of the jet is dissipated through turbulence with no pressure recovery (like in the case of a free jet). Therefore, pressure in the jet is (assuming pressure continuity) the acoustic pressure $p(t)$ imposed by the resonator response to the incoming volume flow u . This model is corroborated by experiments¹⁷. Similar descriptions are used for double-reeds instruments¹ and buzzing lips¹¹.

B. Characteristic equation and instability threshold

The conditions for which self-sustained oscillations become possible are sought, that is, for a given configuration of the experiment (ω_r , q_r and L being fixed), the minimum value of blowing pressure required for the static regime to be unstable is investigated. Common linear stability analysis methods²⁴ are used in this study, and solutions having time dependence $\exp(j\omega t)$ are sought. Cancellation of the imaginary part of ω corresponds to

an oscillation that is neither damped nor amplified: it characterizes the instability threshold of static regime. Attention is drawn to the fact that this quantity may differ from the oscillation threshold. As a language abuse this later is often used instead of the former. In Section IV.B, the nature of the bifurcation is studied.

Assuming small vibrations around equilibrium state (mean values of y and p are $y_0 - P_m/K$ and 0, respectively), the volume flow relationship (4) is linearized. Dimensionless quantities are introduced here: θ , \mathcal{Y}_e , D are the dimensionless frequency, input admittance and the reed transfer function, respectively.

$$\theta = \frac{\omega}{\omega_r}, \quad \mathcal{Y}_e(\theta) = \frac{Z_c}{Z_e(\theta)} \quad \text{and} \quad D(\theta) = \frac{1}{1 + jq_r\theta - \theta^2}. \quad (5)$$

There are two dimensionless control parameters: γ is the ratio between mouth pressure and the pressure required to completely close the reed channel in static regime, while ζ mainly depends on mouthpiece construction and lip stress on the reed (ζ equals quantity 2β in Ref. 43).

$$\gamma = \frac{P_m}{Ky_0} \quad \text{and} \quad \zeta = Z_c W \sqrt{\frac{2y_0}{K\rho}}. \quad (6)$$

Linearization of Eq. (4) leads to the so-called characteristic equation:

$$\mathcal{Y}_e(\theta) = \zeta \sqrt{\gamma} \left\{ D(\theta) - \frac{1-\gamma}{2\gamma} \right\}, \quad (7)$$

which can be split into real and imaginary parts:

$$\Im \mathfrak{m}(\mathcal{Y}_e(\theta)) = \zeta \sqrt{\gamma} \Im \mathfrak{m}(D(\theta)), \quad (8)$$

$$\Re \mathfrak{e}(\mathcal{Y}_e(\theta)) = \zeta \sqrt{\gamma} \left(\Re \mathfrak{e}(D(\theta)) - \frac{1-\gamma}{2\gamma} \right). \quad (9)$$

At last, a dimensionless length $k_r L = \omega_r L/c$ is introduced.

C. Numerical techniques

The unknowns θ , $\gamma \in \mathbb{R}^+$ satisfying Eq. (7) are numerically determined for a range of bore lengths, parameters (q_r, ζ, ω_r) being set. They correspond to frequency and mouth pressure at instability threshold of the static regime. When various solutions exist for a given configuration due to the interaction of the reed resonance with the several bore resonances, the threshold observed experimentally by increasing the blowing pressure is the one having the minimum value of γ .

The characteristic equation is transcendental and may have an infinite number of solutions. Zero-finding is done using the Powell hybrid method³², which combines the advantages of both Newton methods and scaled gradient ones. A continuation technique is adopted to provide an initial value to the algorithm: the first resolution is done for very high values of L ($k_r L \simeq 30$), i.e. for a nearly dynamicless reed where $f \simeq (2n-1)c/4L$ and $\gamma \simeq 1/3$ (with $n \in \mathbb{N}$). Bore length is then progressively

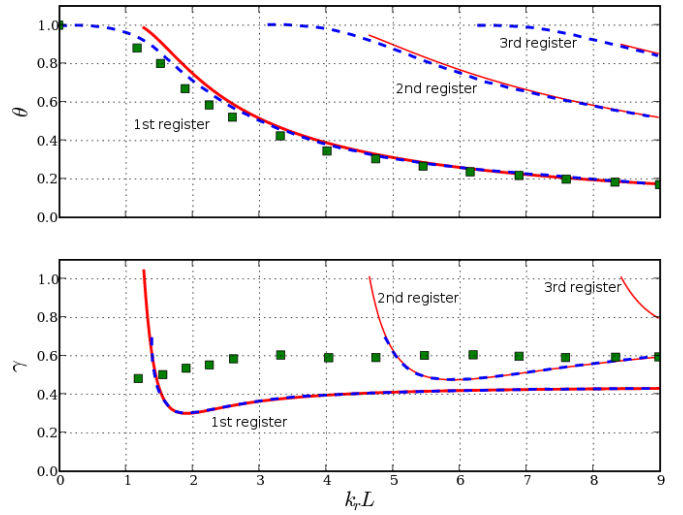


FIG. 1. Dimensionless threshold frequencies (top) and pressure (bottom) for a strongly damped reed: $q_r = 0.4$, $f_r = 750\text{Hz}$, $\beta = 0.065$. Results (dashed lines) and measurements (squares) from Ref. 43; our numerical results (solid lines).

decreased and zero-finding for a given value of L is initialized with the pair (θ, γ) solution of the previous solving (bore slightly longer). Depending on the initialization of the first resolution ($k_r L = 30$), it is possible to explore the branches associated with the successive resonances of the bore. When reed resonance and bore antiresonance get closer to each other ($k_r L \rightarrow n\pi$ ($n \in \mathbb{N}$)), fast variations of the pressure threshold requires to adjust the step size.

D. Results

Two kinds of behaviour can be distinguished. For strongly damped reeds (Figure 1), the threshold frequencies (dashed lines) always lie near both the reed resonance ($\theta = 1$) and the first impedance peak frequency of pipe (hyperbola $\theta = \pi/(2k_r L)$, not represented in Figure for readability), corresponding to the first register of the instrument. When the length L decreases, pressure threshold gradually reduces from values assumed for the dynamicless reed model to a minimum point for $k_r L \sim \pi/2$, and then strongly increases as the pipe becomes shorter. When increasing γ from 0, the loss of stability of the static regime may give rise to an oscillating solution which always corresponds to the first register, since the instability thresholds of the higher registers occur for higher values of mouth pressure. On the contrary, considering now lightly damped reeds (Figure 2), emerging oscillations can occur near higher pipe resonances. Indeed, for certain ranges of L , pressure threshold associated with one particular higher-order register is lower than the pressure required to drive the air column in the other registers. This lowest pressure threshold is associated with the acoustic mode, the natural frequency of which being the closest to the reed resonance.

These results show the influence of reed damping on

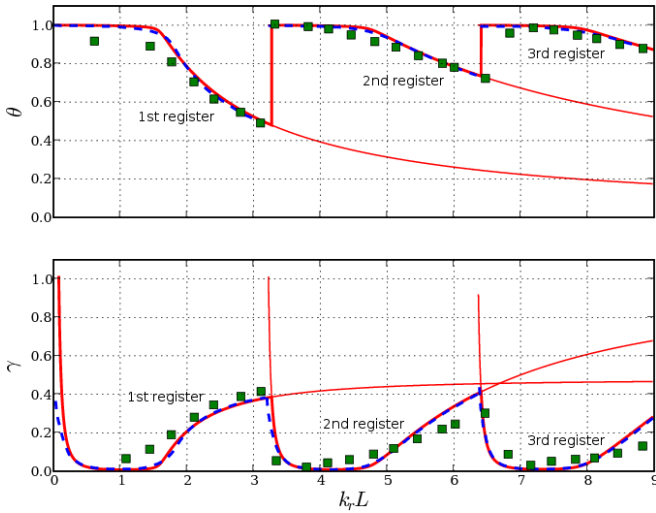


FIG. 2. Dimensionless threshold frequencies and pressure for a lightly damped reed: $q_r = 0.008$, $f_r = 700\text{Hz}$, $\beta = 0.05$. Results (dashed lines) and measurements (squares) from Ref. 43; our numerical results (solid lines).

selecting:

- a clarinet-like behaviour with heavily damped cane reed: preference is given to the *chalmereau* register, i.e. the lowest register,
- or a lingual organ pipe behaviour with very lightly damped metallic reed: tuning is performed by adjusting reed vibrating length by means of a wire adjusted on reed, see Ref. 30 for further details.

This noticeable conclusion of Wilson & Beavers paper gainsays Helmholtz, who states that the differences of behaviour is linked to the mass of reed.

E. Discussion

Despite the important results obtained by WB, discrepancies concerning numerical results and model limits can be pointed out. In a validation phase of our numerical algorithms, our results (see Figures 1 and 2) were compared to their ones (the data being extracted from their article), solving exactly the same equation. Differences appear between numerical results concerning threshold frequencies, approaching reed resonance when length decreases. Assuming a lossless bore $\Re(\mathcal{Y}_e(\omega)) = 0$ in Eqs.(8,9), the condition of positive pressure threshold $\gamma > 0$ leads to the following required inequality:

$$\frac{(1 - \theta^2)^2 + (q_r \theta)^2}{(1 - \theta^2)^2 + (q_r \theta)^2 + 2(1 - \theta^2)} > 0. \quad (10)$$

As a consequence, the denominator needs to be positive too. It accepts two positive solutions θ_1 and θ_2 as well as their opposite. Assuming a second-order approximation in q_r , their expression can be deduced:

$$\theta_1 = 1 + q_r^2/4 \text{ and } \theta_2 = \sqrt{3}(1 - q_r^2/4). \quad (11)$$

For values of θ between these two limits, the system accepts no solution, i.e. no oscillations are possible within this frequency range. Considering bore losses only slightly shifts these limits. This analytical derivation means that frequency threshold would go above ω_r as $\omega_1 = \omega_r \theta_1 = \omega_r(1 + q_r^2/4)$. For heavily damped reeds and very short pipe, one might be able to play much sharper than WB results suggests. Our results were confirmed by a method based on the modal decomposition of the resonator (see section IV.A).

Further investigations pointed out model limits the authors do not take into account: linearization of flow relationship is valid only while reed channel is not closed at rest, i.e. when $P_m < Ky_0$. Using the linear form for higher values of P_m would be meaningless, even for free reed aerophones: the opening function (linked to the reed displacement) taking part in flow calculation can never be negative. For instruments for which reed beats against the mouthpiece, reed channel is completely closed and then sustained oscillations cannot occur for bore length where WB theory predicts pressure threshold above static beating reed pressure, by extending linearization beyond model limits. As a consequence, such considerations do not allow to determine if it is possible to play sharper than reed-lip-mouthpiece system resonance frequency.

F. Minimum pressure threshold: Improved playability for interacting resonances

For each value of q_r , there exists one or more ranges of bore lengths where playability is greatly improved. Indeed, pressure threshold curves show a minimum for a certain value of $k_r L$, denoting an increased easiness to produce the note corresponding to this length. Associating a clarinet mouthpiece with a trombone slide, informal experiments confirm that it is easier to produce some notes than other ones. Analytical approximated expression of this minimum have been investigated. Under the assumption that this minimal value is obtained for an emerging frequency located close to a reed resonance, and therefore is mainly determined by reed damping, bore losses can be ignored $\Re(\mathcal{Y}_e(\omega)) = 0$, Eq. (9) leading thus to:

$$\gamma = \frac{1}{1 + 2\Re(D(\theta))}. \quad (12)$$

In the dynamicless reed model ($D(\theta) = 1$), threshold pressure is equal to 1/3 and frequencies corresponds to frequencies for which the imaginary part of bore input impedance vanishes, which is consistent with results already published²⁷. The minimum pressure threshold occurs at a maximum of $\Re(D(\theta))$:

$$\Re(D(\theta)) = \frac{1 - \theta^2}{(1 - \theta^2)^2 + (q_r \theta)^2}, \quad (13)$$

obtained for $\theta = \sqrt{1 - q_r}$ (which is consistent with the approximation $\theta \simeq 1$), thus:

$$\gamma_0 = \frac{q_r(2 - q_r)}{2 + q_r(2 - q_r)}, \quad (14)$$

nearly proportional to q_r for lightly damped reeds.

Considering now a one-mode resonator with losses:

$$\mathcal{Y}_e(\omega) = Y_n \left(1 + jQ_n \left(\frac{\omega}{\omega_n} - \frac{\omega_n}{\omega} \right) \right), \quad (15)$$

where Y_n is the admittance minimum amplitude and Q_n the quality factor, Eqs. (8,9) become:

$$Y_n + \zeta \frac{1 - \gamma}{2\gamma} = \zeta \sqrt{\gamma} \frac{1 - \theta^2}{(1 - \theta^2)^2 + (q_r \theta)^2} \quad (16)$$

$$Q_n \left(\frac{\theta}{\theta_n} - \frac{\theta_n}{\theta} \right) = -\zeta \sqrt{\gamma} \frac{q_r \theta}{(1 - \theta^2)^2 + (q_r \theta)^2}. \quad (17)$$

Ignoring the variation of Y_n with frequency, the derivation of Eq. (16) with respect to $k_r L$ leads to a minimum value of the function $\gamma = f(k_r L)$ for $\theta_{\min}^2 = 1 - q_r$ and γ_{\min} solution of equation:

$$\frac{Y_n}{\zeta \sqrt{\gamma_{\min}}} + \frac{1 - \gamma_{\min}}{2\gamma_{\min}} = \frac{1}{q_r(2 - q_r)} \quad (18)$$

which first-order solution is given by:

$$\gamma_{\min} \simeq \gamma_0 \left(1 + 2 \frac{Y_n}{\zeta} \sqrt{\gamma_0} \right) \quad (19)$$

obtained for

$$\omega_n = \omega_r \left(1 - \frac{q_r}{2} + \frac{1}{2Q_n} + \frac{\zeta}{2Y_n Q_n \sqrt{q_r}} \right). \quad (20)$$

For an open/closed cylinder $\omega_n = (2n - 1)\pi c/2L$, the result is:

$$(k_r L)_{\min} \simeq (2n - 1) \frac{\pi}{2} \left(1 + \frac{q_r}{2} - \frac{1}{2Q_n} - \frac{\zeta}{2Y_n Q_n \sqrt{q_r}} \right). \quad (21)$$

Typical values $Y_n = 1/25$, $\zeta = 0.4$ and $q_r = 0.4$ lead to an increase of γ_{\min} towards γ_0 of about 8%, confirming the preponderant effect of reed damping on the minimum pressure threshold.

In order to understand how coupling acoustical and mechanical resonances could reduce pressure threshold upon a wider bore length range, the neighborhood of the previously mentioned minimum has been studied. Using again a single acoustical mode for the calculation, derivation of a parabolic approximation was possible. Writing $\gamma = \gamma_{\min}(1 + \varepsilon^2)$, $\theta^2 = \theta_{\min}^2 + \delta$ and $\omega_n = (\omega_n)_{\min}(1 + \nu)$, with ε , δ and ν small quantities, the Taylor expansion of Eqs. (16,17) with respect to these values leads to the next relationships:

$$\varepsilon^2 \sim \delta^2 / (2q_r^2), \quad (22)$$

$$2q_r^2 Y_n Q_n (\delta - 2\nu) = -\delta \zeta \sqrt{q_r}. \quad (23)$$

Finally, near the minimum pressure threshold, dependence to bore length is given by:

$$\gamma = \gamma_{\min} \left(1 + \frac{2q_r}{\left(q_r^{3/2} + \frac{\zeta}{2Y_n Q_n} \right)^2} \left(\frac{k_r L - k_r L_{\min}}{k_r L_{\min}} \right)^2 \right). \quad (24)$$

In a first approximation, the aperture of the approximated parabola, thus the width of the range for which oscillation threshold is lowered, is mainly controlled by the musician embouchure, i.e. by reed damping and lip stress on the reed. This means that, thanks to its embouchure, the player can expect an easier production of tones for certain notes.

For a lossy cylindrical open/closed bore, modal expansion of input impedance gives $Y_n Q_n = \omega_n L / 2c = (2n - 1)\pi/4$, so that bore losses do not seem to have a great influence on playing facility, at least when considering minimal blowing pressure γ_{\min} (Q_n does not appear alone in first order calculation). On the contrary, they are essential for the understanding of the extinction threshold phenomenon¹⁶, i.e. when the reed is held motionlessly against the lay.

III. MODEL IMPROVEMENTS

Last four decades have been fruitful in physical modelling of musical instruments, especially for single reed instruments. Pipes have been the focus of a great number of studies since Benade⁴, as well as the description of peculiarities of flow (Backus³, Hirschberg²⁵, Dalmont *et al.*¹⁷). The aim is here to try to reduce discrepancies between WB experiments and theory, based on some of those investigations which look relevant to the study of oscillation threshold.

A. Visco-thermal losses model and vena contracta

It should be noticed that there is a gap in pressure threshold values between experiment and theory in WB article. This occurs even for long bores, when reed dynamical behaviour should not deviate from the ideal spring model (because of an emerging frequency much smaller than ω_r). For that case, Kergomard *et al.*²⁸ provided an approximated formula taking into account both reed dynamics and bore losses:

$$\gamma \simeq \frac{1 - \theta_n^2}{3 - \theta_n^2} + \frac{2 \Re(\mathcal{Y}_e(\theta))}{3\sqrt{3}\zeta}, \quad \theta_n = (2n - 1) \frac{\pi}{2k_r L}. \quad (25)$$

θ_n corresponding to the n^{th} resonance frequency of the bore. In comparison with ideal model (lossless bore and dynamicless reed, i.e. $\gamma = 1/3$), additional corrective terms are considered in Eq. (25), one lowering pressure threshold due to the collaboration of the resonant reed, the other one requiring higher blowing pressure due to dissipation in the bore. According to this approximated expression, pressure thresholds depend on the mouth-piece parameter and on bore dissipation at playing frequency.

Now focus is done on using realistic values of ζ and $\mathcal{Y}_e(\theta)$, assuming acoustic losses in clarinet-like bore to be due mainly from visco-thermal dissipation (Benade⁴). Others kinds of losses such as nonlinearity localized at the open-end of a tube are negligible since study is done at oscillation threshold, i.e. for very small amplitude oscillations. Simpler model ("Raman's model") has been

recently investigated by Dalmont *et al.*¹⁶ and led to satisfactory oscillation threshold of the fundamental register of the clarinet, when operating frequencies are much lower than reed natural frequency (the reed being considered as an ideal spring). In the present study, the magnitude of the higher order impedance peaks needs to be correctly estimated, so that neither Raman nor Backus³ losses models may be realistic enough. Pressure thresholds would be inaccurate when higher-order modes of bore oscillate first.

The standard formula for the input impedance will be hence considered:

$$\mathcal{Z}_e(\omega) = jZ_c \tan(kL) \text{ with } jk = \frac{j\omega}{c} + \alpha\sqrt{\frac{j\omega}{c}} \quad (26)$$

where α is a coefficient quantifying the visco-thermal boundary layers, equals to 0.0421 for a 7mm radius cylinder. This model introduces dissipation and dispersion, and leads to a zero valued impedance at zero frequency, which is still consistent with the linearization of flow relationship for a zero mean value of acoustic pressure. In this expression, visco-thermal effects are ignored in the characteristic impedance (see Ref. 27). Eq. (26) leads to peaks magnitudes inversely proportional to length L , whereas they are not sensitive to L in Backus empirical expression. A direct consequence is that pressure threshold increases as resonator lengthens.

Another effect may occur and modify pressure threshold. Hirschberg^{25,26} brought to attention on vena contracta phenomenon: due to sharpness of edges, flow separation may result in the formation of a free jet in reed channel, this contraction effect resulting in a jet cross-sectional area smaller than the reed channel opening. Recent investigations¹³ applying the lattice Boltzmann method to the reed channel confirm previous experiments⁴⁰. The assumption of constant vena contracta is valid in some specific cases, for short channel geometry and about half a period for dynamic regimes. Here small vibrations of the reed near oscillation threshold are considered, that may induce little influence of the flow unsteadiness on the measured pressure threshold. So it is possible²⁵ to include vena contracta phenomenon by multiplying the area of the reed channel $Wy(t)$ by a coefficient nearby 0.6, i.e. by multiplying ζ by this coefficient.

Numerical investigations point out (see Figure 3) that taking into account realistic losses and vena contracta phenomenon reduces discrepancies in pressure threshold, especially for high values of bore length and for a strongly damped reed, i.e. when reed dynamics has a small influence on oscillation threshold. Nevertheless pressure values experimentally obtained by WB still remain quite higher than the ones corresponding to the modified model, while frequencies are unaltered.

An attempt to explain the discrepancies in threshold measurements will be provided in section IV.

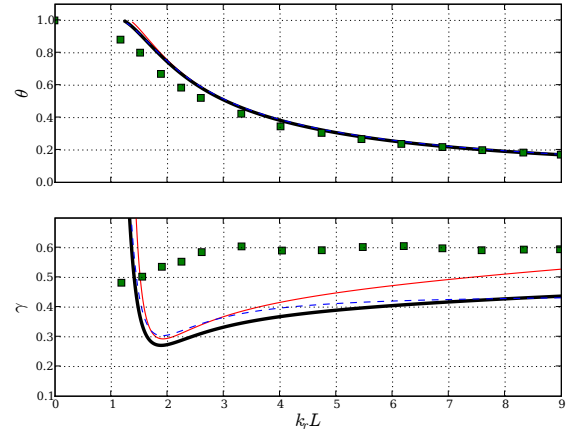


FIG. 3. Results with the model considering vena contracta phenomenon (thin line) and visco-thermal losses (thick line) (same conditions as Figure 1). WB results are also reminded (dashed line).

B. Reed motion induced flow

The influence of the reed is not limited to its resonance. Since Nederveen³¹ and Thompson³⁹, it is proved that flow entering through reed opening is divided in one part exciting the resonator and another part induced by reed motion. In fact, the vibration of the surface of the reed produces an additional oscillating flow. Thus the entering flow U can be written as:

$$U(\omega) = \mathcal{Y}_e(\omega)P(\omega) + S_r(j\omega Y(\omega)), \quad (27)$$

S_r being the effective area of vibrating reed related to the tip displacement $y(t)$. Alternately, a length Δl can be associated to the fictitious volume where reed swings. Dalmont *et al.*¹⁵ reported typical values of 10mm for a clarinet. Nederveen³¹ linked Δl to reed strength (or *hardness*): Δl may approximately vary from 6mm (strong reeds) to 9mm (softer reeds). These values being small compared to clarinet dimensions, reed motion induced flow can be considered through a mere length correction in common work, but its influence on the interaction between acoustic resonator and reed is not negligible on the threshold frequency, as it is studied now.

In a first step, this effect is considered separately, all losses are ignored ($q_r = 0$ and $\alpha = 0$). Eq. (27) coupled to Eq. (7) leads to the following system:

$$-\Im(\mathcal{Y}_e) = k_r \Delta l \frac{\theta}{1 - \theta^2}, \quad (28)$$

$$\frac{1}{1 - \theta^2} - \frac{1 - \gamma}{2\gamma} = 0 \Leftrightarrow \gamma = \frac{1 - \theta^2}{3 - \theta^2}. \quad (29)$$

As seen previously, several frequency solutions θ exists for different pressure thresholds γ . Examination of Eq. (29) as a function $\gamma = f(\theta^2)$ (for $\theta < 1$) reveals that the solution having the lowest threshold is the one being the closest to reed frequency.

Approximations can be derived in some situations. When playing close to a bore resonance frequency $\theta_n \ll 1$, right-hand term in Eq. (28) is small, so that, with $\mathcal{Y}_e = -j \cot(\theta k_r L)$, reed motion induced flow acts merely as a length correction:

$$\Delta l \frac{1}{1 - \theta_n^2} \text{ where } \theta_n = \frac{(2n - 1)\pi}{2k_r L}. \quad (30)$$

This approximation is valid when the considered bore frequency θ_n remains smaller than unity. An equivalent approximated length correction can be derived for the effect of reed damping on frequencies from Eq. (8):

$$\Delta l_q \simeq \zeta \frac{q_r}{\sqrt{3}k_r}. \quad (31)$$

Numerical estimations of length corrections from oscillation frequency exhibit a higher value for the reed motion induced flow ($\Delta l \simeq 12\text{mm}$) than for the reed damping ($\Delta l_q \simeq 2\text{mm}$) in the conditions of Figs. 1 and 5. When acoustical and mechanical resonances are very close ($\theta = 1 - \varepsilon$ and $\theta_n = 1 - \varepsilon_n$), a second-order expression can be deduced:

$$\varepsilon = \frac{\varepsilon_n}{2} \left(1 + \sqrt{1 + 2 \frac{\Delta l}{L \varepsilon_n^2}} \right), \quad (32)$$

the apparition of a square root being typical of mode coupling, making difficult the achievement of analytical expressions. Then, when bore length decreases enough so that one of its resonances increases above reed one ($\theta_n > 1$), the oscillation frequency approaches to the reed one until interception point disappears for $n\pi k_r L = 1$ (see Fig. 4). Near the reed resonance, first-order approximations can be derived:

$$\theta \simeq 1 - \frac{1}{2} k_r \Delta l \tan(k_r L), \quad (33)$$

$$\gamma \simeq \frac{1}{2} k_r \Delta l \tan(k_r L). \quad (34)$$

These expressions are valid if $\tan(k_r L) \gtrsim 0$ i.e. $k_r L \gtrsim n\pi$. According to Eq. (29), when oscillation frequency approaches f_r , the pressure threshold decreases to zero contrary to what happens when considering the reed damping effect.

Figures 5 and 6 show a numerical comparison of the respective effects of reed motion induced flow and reed damping. The first effect adjusts the frequency deviation for both heavily and lightly damped reeds, even when approaching reed resonance, and is preponderant compared to the second one. This justifies classical approaches for the calculation of playing frequencies, ignoring the flow due to pressure drop, and searching for eigenfrequencies of the passive system including the bore and the reed only. It can be noticed that Eq. (28) was already given by Weber⁴² in the early nineteenth century (see page 216), assuming a reed area equal to the cylindrical tube section. This theory, used by several authors (see e.g. Miklos³⁰), was discussed by Helmholtz⁴¹ and Bouasse⁸, especially concerning the lack of explanation concerning the production of self-sustained oscillations. On the contrary,

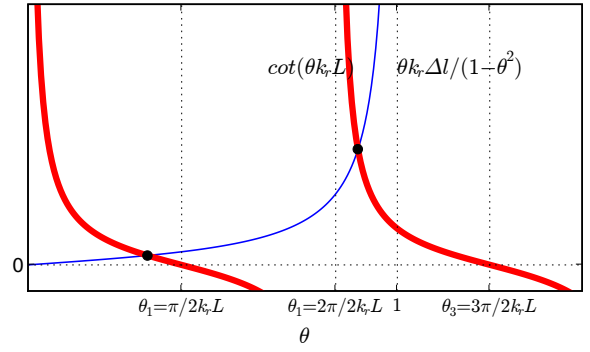


FIG. 4. Graphical representation of Eq. (28) giving oscillation frequency at threshold: left hand term $-\Im(\mathcal{Y})$ (thick lines), right hand term $k_r \Delta l \theta / (1 - \theta^2)$ (thin line) and solutions (markers).

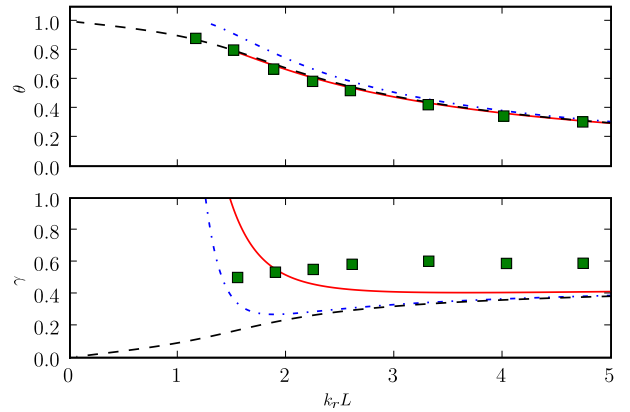


FIG. 5. Comparing reed motion induced flow effect and reed damping effect ($\Delta l = 12\text{mm}$ and other conditions as in Figure 1): reed motion induced flow only (dashed lines), reed damping only (dash-dot lines), both effects (plain lines). WB experimental results are reminded (squares).

threshold pressure curves exhibit that both phenomena have influence on the pressure required for the reed to oscillate. So a combination of damping and additional flow has to be taken into account, none of them being negligible in the considered domain.

IV. GOING BEYOND INSTABILITY THRESHOLD

A. Linear stability analysis with modal decomposition

Analysis of the instability threshold can be performed using complex frequencies formalism. For a given configuration of the whole system *bore-reed-musician* (L , r , ω_r , q_r , γ and ζ being set), its complex eigenfrequencies $s_n = j\omega_n - \alpha_n$ can be determined. The imaginary part of s_n corresponds to the frequency, the real part α_n being the damping of this mode, for the coupled, linearized system close to the static equilibrium state. Classically, when the mouth pressure is below the oscillation threshold, all eigendampings α_n are positive, the static regime

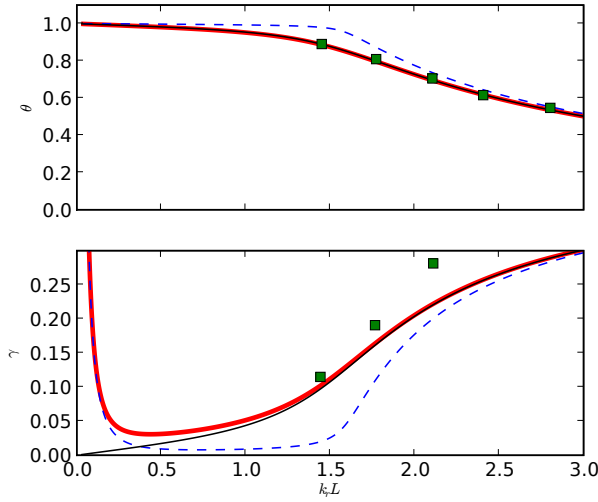


FIG. 6. Comparing reed motion induced flow effect and reed damping effect ($\Delta l = 5\text{mm}$ and other conditions as in Figure 2): reed motion induced flow only (plain thin lines), reed damping only (dashed thin lines), both effects (plain thick lines). WB experimental results are reminded (squares).

being stable. An oscillation may appear when at least one mode of the whole system becomes unstable, i.e. when at least one of the α_n becomes negative. Looking for instability threshold can be done by varying a bifurcation parameter (either L , γ or ζ) and examining the real part of computed eigenfrequencies. Two examples are shown in Figures 7 and 8. It is noticeable that the frequencies evolves only slightly with the bifurcation parameter γ , and are close to eigenfrequencies of either the bore or the reed ($\Im m(j\omega/\omega_r) \simeq 1$). For the first example, static regime becomes unstable for $\gamma \simeq 0.28$ and a frequency near the first resonance of the bore (dot-dashed curves). Other acoustic resonances (their frequencies being odd multiples of first one) and reed resonance have higher oscillation threshold and remain damped for this configuration. For a longer tube (Figure 8), instability appears for $\gamma \simeq 0.3$ at a frequency located near the third resonance of the bore (solid line at $\Im m(j\omega/\omega_r) \simeq 0.8 \simeq 3 * 0.27$), the first resonance becoming unstable for a larger mouth pressure. Frequency close to reed resonance (dot-dashed curves) still remains damped.

Calculations may be simplified and accelerated by using a modal decomposition of the bore impedance $Z_e(\omega)$: this allows for the characteristic equation to be written as a polynomial expression of $j\omega$, and optimized algorithms for polynomial root finding can be used. Modal expansion considers the N first acoustic resonances of the bore:

$$\frac{Z_e(\omega)}{Z_c} = j \tan\left(\frac{\omega L}{c} - j\alpha(\omega)L\right) \quad (35)$$

$$\simeq \frac{2c}{L} \sum_{n=1}^N \frac{j\omega}{\omega_n^2 + jq_n\omega\omega_n + (j\omega)^2} \quad (36)$$

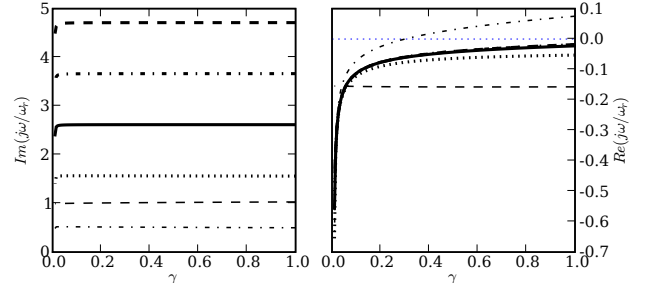


FIG. 7. Evolution of the complex eigenfrequencies as a function of mouth pressure γ . $L = 16\text{cm}$, $r = 7\text{mm}$, $\omega_r = 2\pi \times 1000\text{rad/s}$, $q_r = 0.3$, $\zeta = 0.2$.

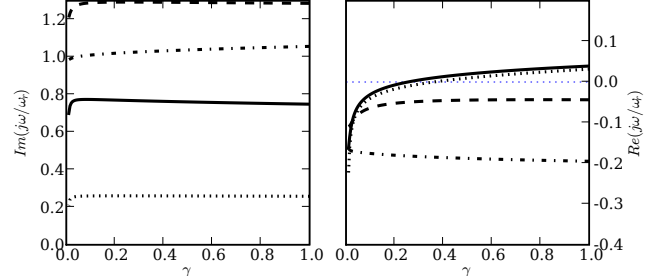


FIG. 8. Evolution of the complex eigenfrequencies as a function of γ . $L = 32\text{cm}$, $r = 7\text{mm}$, $\omega_r = 2\pi \times 1000\text{rad/s}$, $q_r = 0.3$, $\zeta = 0.2$.

where modal coefficients ω_n and q_n can be deduced either from measured input impedance or from analytical expression Eq. (35), assuming $\alpha(\omega)$ to be a slowly varying function of frequency.

Comparison between direct calculation of oscillation threshold γ_{th} using WB method and estimation using modal decomposition and complex eigenfrequencies computing has been done. Whereas the difficulties for the first method arise due to the transcendental characteristic equation, the second one requires calculation of eigenvalues for various values of the mouth pressure γ , using an iterative search of the instability threshold. The number of modes taken into account has been chosen such that resolution of γ_{th} is less than 0.01, which is also the tolerance used for the iterative search. An example is given in Table I for a heavily damped and strong reed. It shows very good agreement between the two methods for both γ and θ . This validation allows the use of the complex frequency approach, which results in an efficient algorithm that can be easily applied to more complex resonator whenever modal description is available.

The writing of the characteristic equation for a single acoustic mode exhibits the behaviour of the coupled

| $k_r L$ | θ_{CF} | θ_{WB} | $\Delta\theta$ | γ_{CF} | γ_{WB} | $\Delta\gamma$ |
|---------|---------------|---------------|----------------|---------------|---------------|----------------|
| 8.5 | 0.185 | 0.186 | 0.5% | 0.43 | 0.43 | 0.1% |
| 2 | 0.747 | 0.747 | 0.1% | 0.30 | 0.30 | 0.6% |
| 1 | 1.022 | 1.024 | 0.2% | 3.86 | 3.82 | 1.0% |
| 0.81 | 1.033 | 1.034 | 0.1% | 8.77 | 8.71 | 0.7% |

TABLE I. Comparison of pressure threshold and oscillation frequency calculated using complex frequency formalism (indexed by CF) and Wilson & Beavers method (WB) for $r = 7\text{mm}$, $\omega_r = 2\pi \times 750\text{rad/s}$, $q_r = 0.4$ and $\zeta = 0.13$.

oscillators:

$$\left[\omega_n^2 + j\omega \left(q_n \omega_n + \frac{c}{L} \zeta \frac{1-\gamma}{\sqrt{\gamma}} \right) - \omega^2 \right] \times [\omega_r^2 + j q_r \omega \omega_r - \omega^2] = j\omega \frac{2c}{L} \omega_r^2 \left(\zeta \sqrt{\gamma} + j\omega \frac{\delta L}{c} \right). \quad (37)$$

Coupling realized by the flow in the reed channel modifies the damping of the acoustic mode: in addition to the usual term (corresponding to visco-thermal losses and eventually radiation), damping is increased by a quantity related to mouth pressure and stress on the reed. This may be regarded to as a resistive acoustic behaviour at the bore entrance.

Assuming a linearized model is still relevant during the growth of oscillations (before the saturation mechanism appears), this approach can be extended to investigate the transient response of the coupled system. Characterizing the degree of instability of the system by $\sigma = \min_n \alpha_n$, the slope of the curve $\sigma = f(\gamma)$ gives an information about the instability degree of the system when mouth pressure is slightly higher than oscillation threshold. A great slope would correspond to a very unstable configuration and a quick growth of oscillation, whereas nearly constant curve would lead to a small amplification coefficient and slowly rising vibrations and then to longer transient attack before stabilization of the magnitude of oscillations. Links between the computed eigenfrequencies of the coupled system presented here and the transient behaviour have still to be investigated.

B. Mouth pressure required to obtain a given (small) amplitude

The previous sections of the paper deal with the stability of the static regime, looking for the condition to make a bifurcation possible. Some developments concerning the existence of oscillating regime above the threshold are derived now. Neither stability of oscillation, nor tone deviation issue will not be discussed here.

Grand *et al.*²² suggested the introduction of the limited Fourier series of pressure in the massless reed case. The technique is the harmonic balance applied to oscillations of small amplitudes. Calculations are done hereafter by taking into account the reed dynamics in the

volume flow relationship, which does not appear in the mentioned paper. Fourier series of volume flow depends on Fourier components of signal $P_m - p(t)$ and $y(t)$. Assuming steady state oscillations with angular frequency ω , the signals are written as:

$$p(t) = \sum_{n \neq 0} p_n e^{nj\omega t}, \quad u(t) = u_0 + \sum_{n \neq 0} \mathcal{Y}_n p_n e^{nj\omega t}, \quad (38)$$

$$y(t) = y_0 (1 - \gamma) + y_0 \sum_{n \neq 0} D_n p_n e^{nj\omega t}, \quad (39)$$

where $\mathcal{Y}_n = \mathcal{Y}_e(n\omega)$ and $D_n = D(n\omega)$ are the values of dimensionless bore admittance and reed dynamics for angular frequency $n\omega$. Volume flow relationship is rewritten as:

$$u^2(t) = \zeta^2 (y(t)/y_0)^2 (\gamma - p(t)). \quad (40)$$

Sustained oscillations of very small amplitude are studied, assuming p_1 is a non-vanishing coefficient considered as a first-order quantity. Notations \mathbf{CE}_n and $\mathbf{F}_{(n)}^m$ are introduced:

$$\mathbf{CE}_n = \mathcal{Y}_n / (\zeta \sqrt{\gamma}) + \frac{1-\gamma}{2\gamma} - D_n, \quad (41)$$

$$\mathbf{F}_{(n)}^m = \mathbf{F}_{(m)}^n = D_n D_m - \frac{1-\gamma}{\gamma} (D_n + D_m) - \frac{\mathcal{Y}_n \mathcal{Y}_m}{\zeta^2 \gamma} \quad (42)$$

Cancellation of \mathbf{CE}_n for given ω and γ means that the characteristic equation (7) is solved for $n\omega$ and γ . Expanding Eq. (40) leads to:

$$0 = \left[\frac{u_0^2}{\zeta^2 \gamma} - (1-\gamma)^2 \right] + 2(1-\gamma) \sum_{n \neq 0} \left[\frac{u_0 \mathcal{Y}_n}{\zeta^2 \gamma (1-\gamma)} - D_n + \frac{1-\gamma}{2\gamma} \right] p_n e^{nj\omega t} - \sum_{n, m \neq 0} \mathbf{F}_{(m)}^n p_n p_m e^{(n+m)j\omega t} + \frac{1}{\gamma} \sum_{n, m, q \neq 0} D_n D_m p_n p_m p_q e^{(n+m+q)j\omega t}. \quad (43)$$

It is here assumed that p_n is of order $|n|$ (with $p_{-n} = p_n^*$) (see e.g. Grand *et al.*²²). Continuous component of volume flow is calculated up to order 2:

$$\begin{aligned} \frac{u_0^2}{\zeta^2 \gamma} &= (1-\gamma)^2 + \sum_{n \neq 0} \mathbf{F}_{\begin{pmatrix} \pm n \\ -n \end{pmatrix}} |p_n|^2 \\ &\quad - \frac{1}{\gamma} \sum_{n, m, n+m \neq 0} D_n D_m p_n p_m p_{n+m}^* \\ &\simeq (1-\gamma)^2 + 2 \mathbf{F}_{\begin{pmatrix} \pm 1 \\ \pm 1 \end{pmatrix}} |p_1|^2 + o(p_1^2) \end{aligned} \quad (44)$$

so that, considering u_0 to be real:

$$u_0 \simeq \zeta \sqrt{\gamma} (1-\gamma) \left[1 + \frac{|p_1|^2 \mathbf{F}_{\begin{pmatrix} \pm 1 \\ -1 \end{pmatrix}}}{(1-\gamma)^2} \right] + o(p_1^2). \quad (45)$$

From Eq. (43), frequency ($N\omega$) is extracted for $N \geq 1$:

$$0 = 2(1 - \gamma) \left[D_N - \frac{1 - \gamma}{2\gamma} - \frac{u_0 \mathcal{Y}_n}{\zeta^2 \gamma (1 - \gamma)} \right] p_N + \sum_{n \neq 0} \mathbf{F}_{(N-n)} p_n p_{N-n} - \frac{1}{\gamma} \sum_{n, m \neq 0} D_n D_m p_n p_m p_{N-n-m}. \quad (46)$$

For $N \geq 2$, Taylor series expansion up to order N is applied: in the first sum, only terms corresponding to $0 \leq n \leq N$ contribute at order N , while, in the second one, the terms to consider are the ones for which $0 < n < N$ and $0 < m < N - n$. The component p_N can be deduced from the sequence $(p_n)_{0 < n < N}$:

$$p_N = \frac{1}{2(1 - \gamma) \mathbf{CE}_N} \left[\sum_{0 < n < N} \mathbf{F}_{(N-n)} p_n p_{N-n} - \frac{1}{\gamma} \sum_{\substack{0 < n < N \\ 0 < m < N-n}} D_n D_m p_n p_m p_{N-n-m} \right] + o(p_1^N). \quad (47)$$

As an example, for $N = 2$, the second sum being empty:

$$p_2 \simeq \frac{\mathbf{F}_{(1)} p_1^2}{2(1 - \gamma) \mathbf{CE}_2} + o(p_1^2). \quad (48)$$

As expected and in agreement with the so-called "Worman rule"⁴⁴, higher components appear to be higher order quantities: order for 2 for p_2 , 3 for p_3 , 4 for p_4 , etc. . .)

Focus is now given to fundamental frequency. Calculations are done up to order 3:

$$0 = 2(1 - \gamma) \left[D_1 - \frac{1 - \gamma}{2\gamma} - \frac{u_0 \mathcal{Y}_1}{\zeta^2 \gamma (1 - \gamma)} \right] p_1 + \sum_{n \neq 0, 1} \mathbf{F}_{(1-n)} p_n p_{1-n} - \frac{1}{\gamma} \sum_{1-n-m, n, m \neq 0} D_n D_m p_n p_m p_{1-n-m} \quad (49)$$

$$\simeq 2(1 - \gamma) \left[D_1 - \frac{1 - \gamma}{2\gamma} - \frac{u_0 \mathcal{Y}_1}{\zeta \gamma (1 - \gamma)} \right] p_1 + 2 \mathbf{F}_{(-2)} p_2 p_1^* - \frac{1}{\gamma} D_1 p_1 |p_1|^2 (D_1 + 2D_1^*)$$

Replacing u_0 and p_2 gives:

$$|p_1|^2 \simeq \frac{2(1 - \gamma)^2 \mathbf{CE}_1}{\frac{\mathbf{F}_{(1)} \mathbf{F}_{(-1)}^{(+2)}}{\mathbf{CE}_2} - \frac{\mathcal{Y}_1}{\zeta \sqrt{\gamma}} \mathbf{F}_{(-1)}^{(+1)} - \frac{1 - \gamma}{\gamma} (D_1^2 + 2|D_1|^2)}. \quad (50)$$

The limitation to the the first harmonic method ignoring the influence of $p_{n \geq 2}$ on the amplitude $|p_1|$ leads to:

$$|p_1|^2 \simeq \frac{2(1 - \gamma)^2 \mathbf{CE}_1}{-\frac{\mathcal{Y}_1}{\zeta \sqrt{\gamma}} \mathbf{F}_{(-1)}^{(+1)} - \frac{1 - \gamma}{\gamma} (D_1^2 + 2|D_1|^2)}. \quad (51)$$

In their paper, Grand *et al.*²² stated that the procedure used in a first simplified case can be applied for a model including reed dynamics provided that $\mathcal{Z}_e(\omega)$ is replaced by $\mathcal{Z}_e(\omega)D(\omega)$. Conclusion is not so straightforward, as reed dynamics also interferes with the volume flow relationship contributing for a more complex expression of the first component amplitude. According to their work, D_n terms would only occur with \mathcal{Y}_n in the expression of $|p_1|^2$ which is not the case.

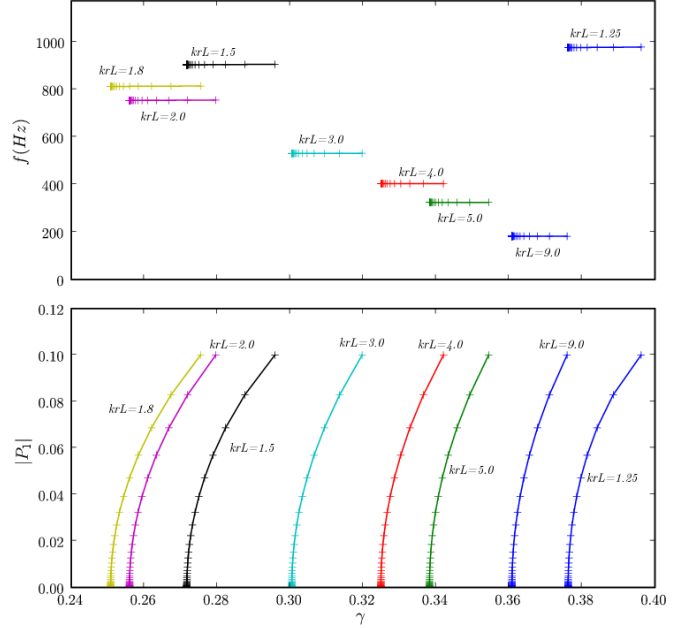


FIG. 9. Comparison of $|p_1|$ computed with the harmonic balance for small oscillations for various values of $k_r L$: from thin to thick lines, $k_r L = 9, 5, 4, 3, 2, 1.8, 1.5, 1.25$ ($\Delta l = 0$, $q_r = 0.4$ and $f_r = 1050\text{Hz}$).

On Figure 9 are shown the bifurcation diagrams for a heavily damped reed. From the flattest tone ($k_r L = 9.00$) to the sharpest computed ($k_r L = 1.25$), oscillations with very small amplitudes are possible as the diagrams show Hopf bifurcation that are supercritical, i.e. direct, for all the computed cases. On the other hand, for cases where oscillation frequency is closed to the reed one (Figure 10), a subcritical Hopf bifurcations occurs for a range of bore length, with a very small pressure threshold linked to the interaction of reed resonance with the second bore resonance: the bifurcation is there inverse.

In accordance with Grand *et al.*²², it appears that the bifurcation is not always direct. There exist configurations for which computed bifurcation diagram shows a subcritical pitchfork, i.e. small oscillations for values of pressure below static regime instability threshold. The boundary between the two cases are not trivial to explore analytically, requiring the mathematical study of the Eq. (50). Alternately numerical exploration of parameter space can lead to some partial observations. One of them is that the bifurcation seems to be direct when oscillation frequency is closed to one of the bore resonance.

The limit of calculations derived here needs to be em-

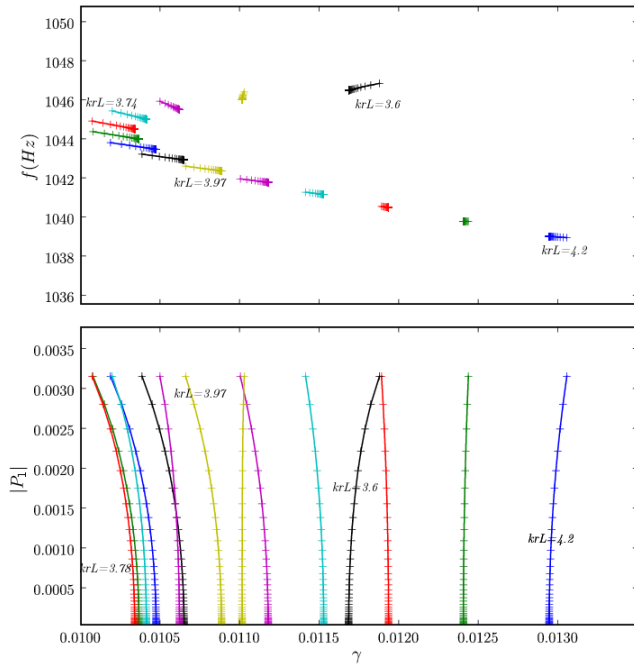


FIG. 10. Comparison of $|p_1|$ computed with the harmonic balance for small oscillations for 14 values of $k_r L$ regularly spaced between 3.6 and 4.20, with a lightly damped reed ($\Delta L = 0$, $q_r = 0.01$ and $f_r = 1050\text{Hz}$).

phasized. When $|p_1|$ tends to zero, the oscillation frequency is the one for which the characteristic equation is solved ($\mathbf{CE}_1 = 0$). Higher components (the second one here at the first order approximation) have a non-negligible influence only if \mathbf{CE}_2 becomes small too when approaching oscillation threshold, i.e. if the characteristic equation accepts the solutions ω and 2ω for two close values of mouth pressure: \mathbf{CE}_1 and \mathbf{CE}_2 are small simultaneously. Inverse bifurcation may occur in the degenerate case of simultaneously destabilization of static regime for a frequency and its octave. This consideration can be extended to the more general case of \mathbf{CE}_1 and \mathbf{CE}_N ($N \geq 2$) cancelling an equal mouth pressure value.

As a conclusion, the nature of the bifurcation depends on the roots of the characteristic equation (7): this generalizes the results of Grand *et al.*²².

V. CONCLUSION AND PERSPECTIVES

Two components of the volume velocity at the input of the resonator act on the oscillation threshold values: the first one is due to the pressure drop between mouth and mouthpiece, while the second one is due to the reed movement. Roughly speaking, the first one has a mainly resistive effect, either passive or active, the second one having a mainly reactive effect. This remark can be related to the behaviour of the threshold pressures and frequencies. Concerning the frequencies, the second effect is preponderant, at least for the cases studied by Wilson

& Beavers, and it can justify the historical method due to Weber⁴² regarding the playing frequencies as eigenfrequencies of a passive resonator. Concerning the pressure thresholds, the flow due to pressure drop is essential, and the model based upon Bernoulli equation used by Wilson & Beavers⁴³ seems to be satisfactory, but taking into account the flow due to reed movement is necessary, and improves the results of the authors, mainly for lightly damped reeds.

Discrepancies between Wilson & Beavers experimental results and numerical ones still remain. Can this be due to the nature of the bifurcation at threshold? For a clarinet-like functioning, i.e. for strongly damped reeds, numerical calculation of small oscillations prove that it is supercritical, confirming the works ignoring reed dynamics, while it is not sure for lightly damped reeds. Further experimental investigations are planned to conclude on the nature of the bifurcation on real clarinets.

Concerning the possible generalization of this work, other kinds of either resonators or reeds should be studied, as e.g. in Tarnopolsky *et al.*³⁸. Some authors of the present paper recently obtained simplified theoretical results for a outward striking reed by using a similar method of investigation based upon a single DOF reed model³⁶. Calculations with several DOFs for the reed remain to do, especially for lip reed instruments (see Cullen *et al.*¹²), even if recent works dedicated to vocal folds have been done (see Rutý³³). Finally, the study of transients sound can be made easier with a good knowledge of the linearized functioning of reed instruments.

Acknowledgments

The study presented in this paper was lead with the support of the French National Research Agency ANR within the CONSONNES project. The authors are grateful to A. Hirschberg and Ph. Guillemain for useful discussion.

- ¹ Almeida, A., Vergez, C., and Caussé, R. (2007). “Quasi-static non-linear characteristics of double-reed instruments”, *J. Acoust. Soc. Am.* **121**, 536–546.
- ² Avanzini, F. and van Walstijn, M. (2004). “Modelling the Mechanical Response of the Reed-Mouthpiece-Lip System of a Clarinet. Part I. A One-Dimensional Distributed Model”, *Acta Acustica* **90**, 537–547.
- ³ Backus, J. (1963). “Small-Vibration Theory of the Clarinet”, *J. Acoust. Soc. Am.* **35**, 305–313.
- ⁴ Benade, A. H. (1976). *Fundamentals of Musical Acoustics*, chapter The Woodwinds: I, 430–464 (Dover Publications, New-York).
- ⁵ Benade, A. H. and Gans, D. J. (1968). “Sound production in wind instruments”, in *Sound Production in Man*, volume 155 of *Ann. New York Acad. Sci.*, 247–263 (New York Academy of Sciences).
- ⁶ Benade, A. H. and Kouzoupis, S. N. (1988). “The clarinet spectrum: Theory and experiment”, *J. Acoust. Soc. Am.* **83**, 292–304.
- ⁷ Blevins, R. D. (2001). *Flow-induced vibration*, updated ed. edition (Krieger Publishing, Krieger Drive, Malabar ,Florida 32950).

- ⁸ Bouasse, H. (1986). *Instruments à vent, Tome 1 (Wind Instruments, Vol. 1)*, first published in 1930 edition (Librairie Scientifique et Technique Albert Blanchard, Paris).
- ⁹ Chan, R. W. and Titze, I. R. (2006). “Dependence of phonation threshold pressure on vocal tract acoustics and vocal fold tissue mechanics”, *J. Acoust. Soc. Am.* **119**, 2351–2362.
- ¹⁰ Chang, Y. M. (1994). “Reed stability”, *J. of Fluids and Structures* **8**, 771–783.
- ¹¹ Chick, J., Bromage, S., Campbell, M., Stevenson, S., and Gilbert, J. (2006). “Motion of the Brass Player’s Lips During Extreme Loud Playing”, in *Actes du 8ème Congrès Français d’Acoustique* (SFA, Tours).
- ¹² Cullen, J. S., Gilbert, J., and Campbell, M. (2000). “Brass Instruments: Linear Stability Analysis and Experiments with an Artificial Mouth”, *Acta Acustica* **86**, 704–724.
- ¹³ da Silva, A. R., Scavone, G. P., and van Walstijn, M. (2007). “Numerical simulations of fluid-structure interactions in single-reed mouthpieces”, *J. Acoust. Soc. Am.* **122**, 1798–1809.
- ¹⁴ Dalmont, J.-P. and Frappé, C. (2007). “Oscillation and extinction thresholds of the clarinet: Comparison of analytical results and experiments”, *J. Acoust. Soc. Am.* **122**, 1173–1179.
- ¹⁵ Dalmont, J.-P., Gazengel, B., Gilbert, J., and Kergomard, J. (1995). “Some Aspects of Tuning and Clean Intonation in Reed Instruments”, *Appl. Acoustics* **46**, 19–60.
- ¹⁶ Dalmont, J.-P., Gilbert, J., Kergomard, J., and Ollivier, S. (2005). “An analytical prediction of the oscillation and extinction thresholds of a clarinet”, *J. Acoust. Soc. Am.* **118**, 3294–3305.
- ¹⁷ Dalmont, J.-P., Gilbert, J., and Ollivier, S. (2003). “Non-linear characteristics of single-reed instruments: Quasi-static volume flow and reed opening measurements”, *J. Acoust. Soc. Am.* **114**, 2253–2262.
- ¹⁸ Elliott, S. J. and Bowsher, J. M. (1982). “Regeneration in brass wind instruments”, *J. Sound Vib.* **83**, 181–217.
- ¹⁹ Fletcher, N. H. (1993). “Autonomous vibration of simple pressure-controlled valves in gas flows”, *J. Acoust. Soc. Am.* **93**, 2172–2180.
- ²⁰ Fletcher, N. H. and Rossing, T. D. (1991). *The Physics of Musical Instruments*, chapter Wind Instruments, 345–494 (Springer).
- ²¹ Gazengel, B., Guimezanes, T., Dalmont, J.-P., Doc, J.-B., Fagart, S., and Léveillé, Y. (2007). “Experimental investigation of the influence of the mechanical characteristics of the lip on the vibrations of the single reed”, in *Proc. Int. Symp. on Musical Acoustics* (Barcelona, Spain).
- ²² Grand, N., Gilbert, J., and Laloë, F. (1997). “Oscillation threshold of woodwind instruments”, *Acta Acustica* **83**, 137, URL <http://hal.archives-ouvertes.fr/hal-00001412/fr/>.
- ²³ Guillemain, P., Kergomard, J., and Voinier, T. (2005). “Real-time synthesis of clarinet-like instruments using digital impedance models”, *J. Acoust. Soc. Am.* **118**, 483–494.
- ²⁴ Hale, J. K. and Kocak, H. (1991). *Dynamics and Bifurcations* (Springer-Verlag, New York).
- ²⁵ Hirschberg, A. (1995). *Mechanics of Musical Instruments*, chapter 7, 291–369, number 355 in CISM Courses and Lectures (Springer, Wien - New York).
- ²⁶ Hirschberg, A., van de Laar, R. W. A., Marrou-Maurières, J.-P., Wijnands, A. P. J., Dane, J. H., Kruijswijk, S. G., and Houtsma, A. J. M. (1990). “A quasi-stationary model of air flow in the reed channel of single-reed woodwind instruments”, *Acustica* **70**, 146–154.
- ²⁷ Kergomard, J. (1995). *Mechanics of Musical Instruments*, chapter 6, 229–290, number 355 in CISM Courses and Lectures (Springer, Wien - New York).
- ²⁸ Kergomard, J., Ollivier, S., and Gilbert, J. (2000). “Calculation of the Spectrum of Self-Sustained Oscillators Using a Variable Truncation Method: Application to Cylindrical Reed Instruments”, *Acta Acustica* **86**, 685–703.
- ²⁹ Lopez, I., Hirschberg, A., van Hirtum, A., Ruty, N., and Pelorson, X. (2006). “Physical Modeling of Buzzing Artificial Lips: The Effect of Acoustical Feedback”, *Acta Acustica* **92**, 1047–1059.
- ³⁰ Miklos, A., Angster, J., Pitsch, S., and Rossing, T. D. (2006). “Interaction of reed and resonator by sound generation in a reed organ pipe”, *J. Acoust. Soc. Am.* **119**, 3121–3129.
- ³¹ Nederveen, C. J. (1998). *Acoustical aspects of woodwind instruments* (Northern Illinois).
- ³² Powell, M. J. D. (1970). *Numerical Methods for Nonlinear Algebraic Equations*, chapter A Hybrid Method for Nonlinear Equations, 87–144 (Gordon and Breach, London).
- ³³ Ruty, N. (2007). “Modèles d’interactions fluide parois dans le conduit vocal. applications aux voies et aux pathologies (Fluid walls interactions modelling in the vocal tract. applications to voice and pathologies)”, Ph.D. thesis, INPG Grenoble.
- ³⁴ Saneyoshi, J., Teramura, H., and Yoshikawa, S. (1987). “Feedback oscillations in reed woodwind and brasswind instruments”, *Acustica* **62**, 194–210.
- ³⁵ Schumacher, R. T. (1981). “Ab initio calculations of the oscillation of a clarinet”, *Acustica* **48**, 71–85.
- ³⁶ Silva, F., Kergomard, J., and Vergez, C. (2007). “Oscillation thresholds for “striking outwards” reeds coupled to a resonator”, in *Proc. Int. Symp. on Musical Acoustics* (Barcelona, Spain).
- ³⁷ Steinecke, I. and Herzog, H. (1995). “Bifurcations in an asymmetric vocal-fold model”, *J. Acoust. Soc. Am.* **97**, 1874–1884.
- ³⁸ Tarnopolsky, A. Z., Fletcher, N. H., and Lai, J. C. S. (2000). “Oscillating reed valves—an experimental study”, *J. Acoust. Soc. Am.* **108**, 400–406.
- ³⁹ Thompson, S. C. (1979). “The effect of the reed resonance on woodwind tone production”, *J. Acoust. Soc. Am.* **66**, 1299–1307.
- ⁴⁰ van Zon, J., Hirschberg, A., Gilbert, J., and Wijnands, A. P. J. (1990). “Flow through the reed channel of a single reed music instrument”, *J. Phys., Colloque de Physique* **51**, sup.2 C2–821–824.
- ⁴¹ von Helmholtz, H. (1954). *On the theory of pipes*, chapter App. VII, 388 (Dover Publications, Inc., New York).
- ⁴² Weber, W. (1829). “Theorie der zungenpfeifen (theory of reed pipes)”, *Annalen der Physik und Chemie*, hrsg. von J.C. Poggendorf **93**, 193–246.
- ⁴³ Wilson, T. A. and Beavers, G. S. (1974). “Operating modes of the clarinet”, *J. Acoust. Soc. Am.* **56**, 653–658.
- ⁴⁴ Worman, W. E. (1971). “Self-sustained nonlinear oscillations of medium amplitude in clarinet-like systems”, Ph.D. thesis, Case Western Reserve University.